Estimation of stand volume by fusing low laser-sampling density LiDAR data with QuickBird panchromatic imagery in closed-canopy Japanese cedar (*Cryptomeria japonica*) plantations

Tomoaki Takahashi[1], Yoshio Awaya[2], Yasumasa Hirata[3], Naoyuki Furuya[4], Toru Sakai[5] & Atsushi Sakai[6]

[1]Forestry and Forest Products Research Institute, 1, Matsunosato, Tsukuba, Ibaraki, 305-0044, Japan, tomokun@ffpri.affrc.go.jp
[2]Forestry and Forest Products Research Institute, 1, Matsunosato, Tsukuba, Ibaraki, 305-0044, Japan, awaya@ffpri.affrc.go.jp
[3]Forestry and Forest Products Research Institute, 1, Matsunosato, Tsukuba, Ibaraki, 305-0044, Japan, hirat09@ffpri.affrc.go.jp
[4] Japan International Research Center for Agricultural Sciences, 1-1, Ohwashi, Tsukuba, Ibaraki 305-8686, Japan, nfuruya@affrc.go.jp
[5]Forestry and Forest Products Research Institute, 1, Matsunosato, Tsukuba, Ibaraki, 305-0044, Japan, torus@ffpri.affrc.go.jp
[6]Japan International Research Center for Agricultural Sciences, 1-1, Ohwashi, Tsukuba, Ibaraki 305-8686, Japan, golgo@affrc.go.jp

Abstract

This study investigated the potential of fusing low laser-sampling density LiDAR data with QuickBird panchromatic imagery for estimating stand volumes. The study area was in closed-canopy, mountainous Japanese cedar (*Cryptomeria japonica*) plantations in Japan. Stand volume in the area ranged from 250.5 to 913.1 m^3/ha and terrain was undulating with an elevation ranging from 135 to 391 m above sea level. A total of 13 circular sample plots (0.04 ha) were established and stand volume within the plots was measured as validation data for evaluating stand volume estimates derived from the fused data through a regression model. The independent variables of the empirical model were individual tree height and crown projection area and the dependent variable was individual stem volume of Japanese cedar. To estimate stand volume with the fused data, LiDAR-derived tree heights and panchromatic imagery-derived crown projection areas were computed for individual tree crowns delineated by the Voronoi tessellation. All results of this study revealed that fusing low laser-sampling density LiDAR data (e.g. 1 point/4 m^2) with QuickBird panchromatic imagery (0.6-m resolution) would have great potential to estimate stand volume precisely in Japanese cedar plantations regardless of different footprint sizes (e.g. 0.16–0.47 m).

Keywords: LiDAR, QuickBird, panchromatic, data fusion, Voronoi tessellation

1. Introduction

Many previous studies have revealed that small-footprint airborne scanning LiDAR (Light Detection and Ranging) can estimate or measure tree and canopy heights accurately in a variety of forest types (e.g. Hyyppä *et al*. 2001; Næsset 2002; Persson *et al*. 2002; Popescu *et al*. 2002; Holmgren *et al*. 2003; Yu *et al*. 2004; Takahashi *et al*. 2005a, 2008a). Although acquisition of high laser-sampling density LiDAR data (e.g. over 10 points/m^2) in vast forests is expensive, such data can provide accurate information on individual tree numbers and crown properties such as diameter and projection area of upper-storey trees. Some research has shown the feasibility of estimating stem or stand volumes accurately from LiDAR-derived tree heights and crown properties in some coniferous forests (Hyyppä *et al*. 2001; Persson *et al*. 2002; Holmgren *et al*. 2003; Takahashi *et al*. 2005b). Although the number of detected trees and the measurement accuracy of the properties apparently deteriorate with decreasing laser-sampling density, the estimates of tree heights with varying laser-sampling density data (i.e. laser shot spacing ranging from less than a meter to a few meters) reported in much of the previous research seem to be comparable with field-measured tree heights. In contrast, high spatial resolution satellite imagery with less than 1-m resolution, such as IKONOS and QuickBird panchromatic images, can cover local/regional scale forests with fine spatial resolution. As QuickBird panchromatic imagery has approximately 0.6-m resolution at nadir, there is a possibility of extracting by image processing individual tree crown properties for upper-storey trees with crown diameters exceeding approximately 1.8 m. Therefore, laser shots of at least approximately 1 point/4 m^2 could hit each crown that can be identified in the panchromatic imagery and so provide approximate estimates of individual tree heights. Assuming that fusion of such low laser-sampling density data with the panchromatic imagery has potential to estimate stem and stand volumes adequately, we therefore attempted to estimate by data fusion stand volumes of Japanese cedar (*Cryptomeria japonica*) plantations in a variety of stand conditions.

In this study, we investigated (1) the potential of high-laser sampling density LiDAR data alone for stand volume estimation and (2) the potential of fusing low laser-sampling density LiDAR data with a QuickBird panchromatic imagery for stand volume estimation. Because laser footprint sizes might affect the tree height estimation (Yu *et al*. 2004; Andersen *et al*. 2006; Takahashi *et al*. 2008b), LiDAR data with different footprint sizes were used for the investigation of (2). A previously constructed regression model whose independent variables were individual tree height and crown projection area and whose dependent variable was individual stem volume of Japanese cedar (Takahashi *et al*. 2005b) was used to estimate stand volumes.

2. Method

2.1 Study area

The study area of approximately 75.2 ha was located in a national forest in Ibaraki Prefecture in central Japan (lat. 36˚ 10’ N, long. 140˚ 10’ E). More than 80% of the area is dominated by plantations of evergreen coniferous Japanese cedar and hinoki cypress (*Chamaecyparis obtusa*) trees, with the remainder dominated by several broadleaved deciduous tree species. Stand age in the coniferous forests ranged from 20 to 100 years. Terrain is undulating with an elevation ranging from 135 to 391 m above sea level. During the fall and winter of 2006, we established 13 circular sample plots (0.04 ha) within the closed-canopy Japanese cedar plantations. All plots consisted purely of planted Japanese cedar and dense understorey vegetation consisting of *Aucuba japonica* and *Eurya japonica*, which are evergreen shrubs with a height of less than approximately 3–5 m.

To locate the center of each sample plot, global positioning system (GPS) surveys were conducted under the static survey performance using a single-frequency ProMark2 receiver (Magellan, Santa Clara, CA, U.S.A.). Details of the GPS surveys are shown in Takahashi *et al*. (2008b). Within each sample plot, all trees with a diameter at breast height (DBH) > 4 cm were callipered. Tree heights were measured for sample trees within plots in young and middle-aged forests using a Häglof Vertex hypsometer (Häglof, Langsele, Sweden). For the young and middle-aged forests, the sample trees (> 50% of the trees within each plot) were selected with equal probability. Next, height-diameter curves were produced for each plot and unmeasured tree heights were estimated from each model. In mature forests, tree heights of all standing trees within each plot were measured using the hypsometer. Trees with heights exceeding the arithmetic mean tree height within each plot were regarded as dominant trees in the present study. Individual stem volumes were calculated from tree height and DBH using standard two-way volume equations for Japanese cedar (Forestry Agency, Japan, 1970). Finally, stand volume (m^3/ha) in each plot was calculated by summing stem volumes of all standing trees within each plot. Summary statistics for 13 field sample plots are shown in Table 1.

Table 1: Summary of field plot data

Plot	A	B	C	D	E	F	G	H	I	J	K	L	M
Stand age	20	20	23	25	25	29	40	41	43	59	59	100	100
Stand density (trees/ha)	2000	1725	2800	2675	2725	1375	1200	2125	475	925	875	1075	1050
No. of trees	80	69	112	107	109	55	48	85	19	37	35	43	42
No. of dominant trees	49	36	57	53	58	24	29	49	9	16	19	21	22
Mean DBH (cm)	17.9	16.3	13.9	16.6	17.0	22.1	25.2	16.4	37.1	29.5	31.0	28.9	26.6
Basal area (m^2/ha)	52.8	37.6	44.0	61.2	65.1	55.3	62.9	47.1	54.1	65.3	71.3	76.8	62.8
Mean tree height (m)	13.9	13.5	10.8	14.3	14.5	19.3	20.8	12.6	24.8	22.6	23.6	24.6	22.6
Dominant tree height (m)	14.9	14.7	11.5	15.4	15.4	20.7	22.4	13.4	26.4	24.4	25.1	26.8	24.5
Stand volume (m^3/ha)	387.1	270.3	250.5	461.5	490.6	539.0	653.8	310.8	605.3	725.3	794.8	913.1	700.0

2.2 LiDAR data

The LiDAR data used in the analysis were those of Takahashi *et al*. (2008b), acquired on 31 August 2006 by Aero Asahi Co., Ltd., Japan. A helicopter-borne laser scanner (Optech ALTM 3100), which is a multi-return system that also collects intensity data, was used. The study site was sampled at three different flight altitudes; 500 m, 1000 m and 1500 m above ground level (a.g.l.). The beam divergence of 0.31 mrad produced footprint diameters of 0.16 m, 0.31 m and 0.47 m, respectively. At each flight altitude, several parallel flight paths were recorded to cover the entire area with average overlapping of 64% between adjacent flight paths. Transmitted laser pulses with scan angles exceeding 8° were excluded from the final analysis to avoid the inclusion of inferior quality data at the edge of strips. Although the laser-sampling densities were approximately 57, 25 and 9 points/m^2, respectively, at each flight altitude, the densities of all datasets were thinned out and finally converted into approximately 1 point/4 m^2. The 57 points/m^2 dataset at 500-m flight altitude was defined as the high-density LiDAR dataset and the 1 point/4 m^2 datasets at three flight altitudes were defined as the low-density LiDAR datasets.

2.3 Processing high-density LiDAR data for delineating individual tree crowns and estimating stand volumes

The high-density (57 points/m^2) LiDAR dataset was used to create a canopy height model (CHM) with a pixel size of 0.25 m (see Figure 1). The CHM was generated by subtracting a digital terrain model (DTM) from a digital surface model (DSM) produced by assigning the height value of the highest laser reflection point within each pixel using only first pulse data.

The DTM was generated by a conventional human-assisted method in which an operator visually inspected the elevations of the DTM after an initial automated filtering (Takahashi *et al.* 2008b). Hereafter, the DTM is defined as DTM_{ref}. Through refining by the maximum filter with variable window sizes (3 x 3 window for CHM ≤ 20 m; 5 x 5 window for CHM > 20 m) and smoothing with a 3 x 3 low-pass filter (Hyyppä *et al.* 2001) for the CHM, the watershed method (e.g. Wang *et al.* 2004) was then applied to delineate individual tree crowns. Next, individual tree stem volume was estimated using the regression model presented in Takahashi *et al.* (2005b). The empirical model consisted of LiDAR-derived tree height and crown projection area as follows:

$$\ln V = \ln \beta_0 + \beta_1 \ln H + \beta_2 \ln CA \qquad (1)$$

where V (m^3) is estimates of individual stem volume, H (m) is LiDAR-derived tree height, and CA (m^2) is LiDAR-derived crown projection area. The values of $\ln \beta_0$, β_1 and β_2 were –8.312, 2.282 and 0.389, respectively. Adjusted coefficient of determination of the model was 0.734. The value of H was assigned to the highest value of the CHM within each segmented crown and the value of CA was the segmented crown area. Finally, stand volume estimates (m^3/ha) in each plot were calculated by summing the individual stem volume estimates of all segmented trees within each plot.

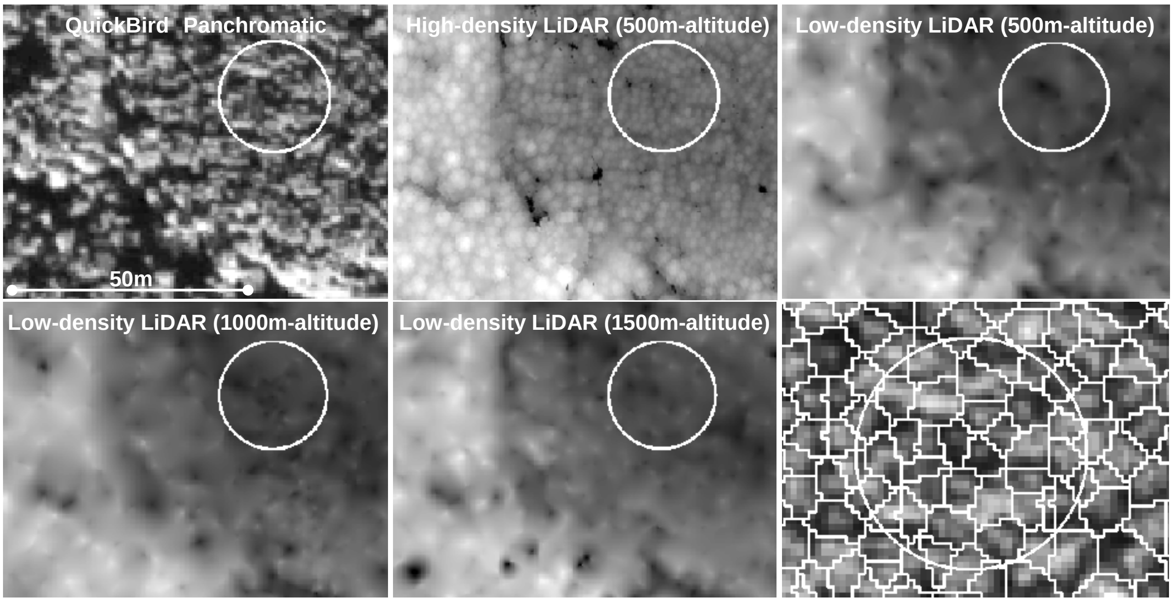

Figure 1: The images of QuickBird panchromatic (0.6-m resolution) and canopy height models (0.25-m resolution) derived from different flight altitude LiDAR data. High and low-densities are approximately 57 points/m^2 and 1 point/4 m^2, respectively. The circle denotes plot C (0.04 ha; 11.28 m radius) and the segmented individual tree crowns were produced by the Voronoi tessellation on the panchromatic imagery.

2.4 Processing low-density LiDAR data and panchromatic imagery for delineating individual tree crowns and estimating stand volumes

The low-density (1 point/4 m^2) LiDAR datasets at three flight altitudes were used to create CHMs with a pixel size of 0.25 m (see Figure 1). To create the CHMs, DSMs were created through interpolation by the natural neighbour method (Bater and Coops 2006). Because the number of ground return laser data was poor at all flight altitudes in the study area, as shown in Takahashi *et al.* (2008b), it was difficult to distinguish ground return laser data from overstorey and understorey vegetation return laser data. Therefore, in the present study, if the difference between the elevation of a given laser data in each altitude dataset and the elevation of the

DTM_{ref} at the same horizontal location did not exceed 1 m (absolute value), then such laser data were regarded as ground return data. DTMs at all flight altitudes were then created through interpolation by the natural neighbour method.

The panchromatic imagery (11-bit data) used in the analysis was acquired on 4 February 2006. The imagery was orthorectified using both the CHM derived from the high-density LiDAR dataset as ground control points (GCP) and a digital elevation model (DEM). The resampling method used in the orthorectification was the cubic convolution method and the resolution of the orthorectified imagery was 0.6 m. Through refining by a 3 x 3 median filter and 3 x 3 local maximum filtering (Wulder *et al*. 2000) to detect local maximum pixel, which can be regarded as individual tree apex or near apex pixel, the Voronoi tessellation (e.g. Worboys and Duckham 2004) was then applied to delineate individual tree crowns (see Figure 1). Next, individual tree stem volumes were estimated by using equation (1). The value of H was assigned to the highest value of the CHMs within each segmented crown on the panchromatic imagery and the value of CA was the segmented crown area. Finally, stand volume estimates (m^3/ha) in each plot were calculated by summing the individual stem volume estimates of all segmented trees within each plot. In addition to fusing these low-density LiDAR datasets with the panchromatic imagery, the high-density LiDAR dataset were also fused with the panchromatic imagery to investigate the effects on the volume estimation of height difference between the low- and high-density LiDAR datasets.

2.5 Validation of stand volume estimates

Before evaluating stand volume estimates, we first investigated the number of detected tree crowns derived from the high-density LiDAR dataset and the panchromatic imagery. The biases and root mean square errors (RMSE) of the dominant mean tree height estimates were computed. Next, to evaluate the accuracy and precision of the stand volume estimates, the systematic errors (i.e. bias), random errors and RMSEs were computed. The relationships between field-measured and estimated stand volumes were investigated by regression analysis, in which models were fitted to the data using the least-squares method.

3. Result

Table 2: Number of detected tree crowns derived from high-density LiDAR data and QuickBird panchromatic imagery

Plot	A	B	C	D	E	F	G	H	I	J	K	L	M
LiDAR-detected	61	59	66	63	65	39	31	56	20	25	27	20	24
QB-detected	27	30	32	29	34	23	21	27	21	21	25	20	24

High density means 57 points/m^2. QB denotes QuickBird imagery. The watershed and Voronoi tessellation methods were applied for the high-density LiDAR data (0.25-m resolution) and the panchromatic imagery (0.6-m resolution), respectively.

The number of detected tree crowns derived from the high-density LiDAR dataset and the panchromatic imagery is shown in Table 2. The differences in the number of detected crowns between the two sets of data are large in dense forests (more than 1200 trees/ha) and small in non-dense forests (less than 1200 trees/ha). The errors in dominant tree height estimates are shown in Table 3. Both the high- and low-density LiDAR datasets underestimated dominant mean tree heights. The tree height estimates with each low-density LiDAR dataset were approximately 1 m less than those derived from the high-density LiDAR dataset.

The errors of stand volume estimates are shown in Table 4. The systematic errors of the estimates were negative values for all datasets. As seen in Figures 2 and 3 and Table 4, the random errors were small for all datasets and there was a strong liner relationship between field-measured and estimated stand volumes for all datasets. According to the regression analysis, the slopes for all regression equations could be regarded statistically as one ($p < 0.05$).

Table 3: Errors of dominant tree height estimates (m)

		Bias	RMSE
High-density LiDAR	(500 m a.g.l.)	-0.69	1.19
Low-density LiDAR	(500 m a.g.l.)	-1.47	2.09
Low-density LiDAR	(1000 m a.g.l.)	-1.85	2.61
Low-density LiDAR	(1500 m a.g.l.)	-1.60	2.27

High and low-densities mean 57 points/m^2 and 1 point/4 m^2, respectively. QB denotes QuickBird imagery and the parenthetic values denote flight altitudes.

Table 4: Errors of stand volume estimates (m^3/ha) and the results of regression analysis

	Systematic error	Random error	RMSE	RMSEr	Slope	Intercept	Ajusted R^2
High-density LiDAR (500 m a.g.l.)	-47.2	46.9	66.6	12.2 %	0.880**	18.52 NS	0.946
QB + high-density LiDAR (500 m a.g.l.)	-124.5	57.5	137.2	25.1 %	0.989**	-118.64*	0.915
QB + low-density LiDAR (500 m a.g.l.)	-182.3	44.1	187.5	34.3 %	0.899**	-126.88**	0.951
QB + low-density LiDAR (1000 m a.g.l.)	-200.1	44.8	205.1	37.5 %	0.861**	-123.98**	0.957
QB + low-density LiDAR (1500 m a.g.l.)	-188.8	42.0	193.4	35.4 %	0.878**	-122.17**	0.960

High and low-densities mean 57 points/m^2 and 1 point/4 m^2, respectively. QB denotes QuickBird imagery and the parenthetic values denote flight altitudes. RMSEr means a relative RMSE divided by average field-measured stand volume. ** ($p < 0.01$); * ($p < 0.05$); NS ($p > 0.05$)

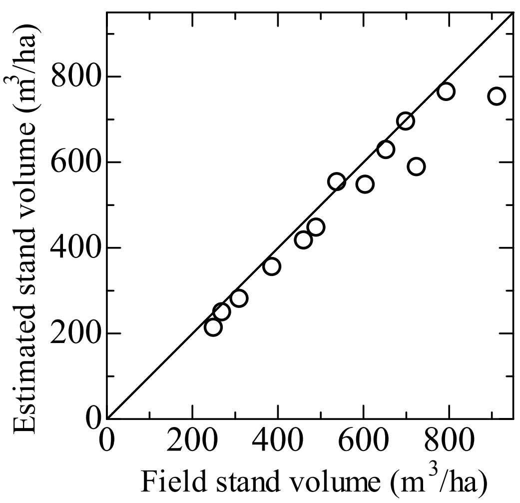

Figure 2: The relationship between field-measured and estimated stand volumes from high-density LiDAR data

4. Discussion

Figure 2 and Table 4 indicate that the high-density LiDAR dataset could estimate stand volumes accurately. Although the number of LiDAR-detected tree crowns was less than the number of field-measured tree crowns, the sum of individual stem volumes estimated by the regression model could explain most of the total volumes within each plot, except for two plots (plots J and L). This result indicates that a large portion of the LiDAR-detected trees had larger individual stem volumes than the undetected trees in each plot. Moreover, these results indicate that the empirical model (Eq. 1) is very useful for estimating stand volumes of Japanese cedar stands with a variety of stand conditions in Japan, despite the model having been constructed within a restricted forest area (stand density; 800–1227 trees/ha, stand volume; 504.8–602.9 m^3/ha). One weakness in the present study is that only 13 field plots were used although the 13 plots cover a good range (250.5–913.1 m^3/ha). We should have increased the number of field sample plots to examine the variability of volume estimates among plots with nearly the same volume.

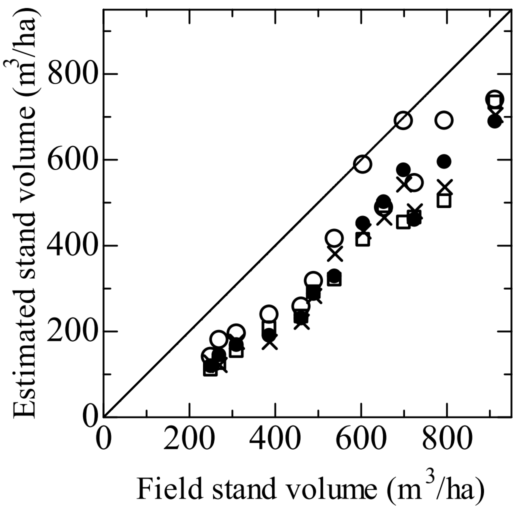

Figure 3: The relationship between field-measured and estimated stand volumes from fused data. Solid circles, 500-m low-density data; square, 1000-m low-density data; cross, 1500-m low-density data; open circles, 500-m high-density data

By contrast, all the fused datasets produced large negative systematic errors in the estimates of stand volumes, although the random errors were as small as those of the non-fused LiDAR datasets. As seen from Figure 3, the dataset (open circles) made by fusing the high-density LiDAR dataset with the panchromatic imagery hardly improved estimates of stand volumes in plots A, B, C, D, E and H (stand volume < 500 m^3/ha: dominant mean tree height < 16 m), whose crown numbers detected by the panchromatic imagery were almost half those detected by LiDAR; however, the fused dataset improved the estimates of stand volumes in some plots (stand volume > 500 m^3/ha: dominant mean tree height > 20 m) whose crown numbers detected by the panchromatic imagery were similar to those detected by LiDAR. This result indicates that the cause of the negative systematic errors in the three fused datasets would be based on an interaction of the omission errors of panchromatic imagery-detected crown numbers (Table 2), the underestimations of LiDAR-derived tree heights (Table 3), and the characteristic/behavior of the logarithmic regression model. Although the reason why the slopes of all regression equations of the fused datasets were regarded statistically as one remains unknown, the three fused datasets could provide almost the same accuracy of stand volume estimates in this study area. These results demonstrate that high-density LiDAR is not needed for all applications, such as estimation of stand volume, especially when fused with other optical remote sensing technologies and over large areas. Also, there seems to be a misconception that one needs near perfect one-to-one correspondence between field data and those predicted empirically from LiDAR.

All results of this study revealed that data fusion of low laser-sampling density LiDAR data (e.g. 1 point/4 m^2) with QuickBird panchromatic imagery would have a great potential for estimating stand volume precisely in Japanese cedar plantations regardless of different footprint sizes (e.g. 0.16–0.47 m). Moreover, if the systematic errors in the estimates were revealed as site-independent values, we would be able to estimate stand volume accurately and precisely with LiDAR data acquisition at a lower cost in vast Japanese cedar forests by using methods presented in this study.

Acknowledgements

We thank Kenichi Shibuya and Kouji Oomori from Aero Asahi Co., Japan for planning the flight and acquiring the LiDAR data. Many thanks to two anonymous reviewers for providing valuable comments on the original manuscript.

References

Andersen, H.E., Reutebuch, S.E. and McGaughey, R.J., 2006. A rigorous assessment of tree height measurements obtained using airborne lidar and conventional field methods. *Canadian Journal of Remote Sensing*, 32, 355-366.

Bater, C.W. and Coops, N.C., 2006. Comparing interpolation algorithms for deriving digital elevation models from unevenly distributed LiDAR ground returns. *Proceedings of the international conference Silvilaser2006*, 43-48.

Forestry Agency, 1970. Timber volume table (Western Japan) (in Japanese). Nihon Ringyo Chosakai, Tokyo, Japan, 13.

Holmgren, J., Nilsson M. and Olsson, H., 2003a. Estimation of tree height and stem volume on plots using airborne laser scanning. *Forest Science,* 49, 419-428.

Hyyppä, J., Kelle, O., Lehikoinen, M. and Inkinen, M., 2001. A segmentation-based method to retrieve stem volume estimates from 3-D tree height models produced by laser scanners. *IEEE Transactions on Geoscience and Remote Sensing,* 39, 969-975.

Næsset, E. and Økland, T., 2002. Estimating tree height and tree crown properties using airborne scanning laser in a boreal nature reserve. *Remote Sensing of Environment*, 79, 105-115.

Persson, A., Holmgren, J. and Soderman, U., 2002. Detecting and measuring individual-trees using an airborne laser scanner. *Photogrammetric Engineering and Remote Sensing*, 68, 925-932.

Popescu, S.C., Wynne, R.H. and Nelson, R.F., 2002. stimating plot-level tree heights with lidar: local filtering with a canopy-height based variable window size. *Computers and Electronics Agriculture*, 37, 71-95.

Takahashi, T., Yamamoto, K., Senda, Y. and Tsuzuku, M., 2005a. Estimating individual-tree heights of sugi (Cryptomeria japonica D. Don) plantations in mountainous areas using small-footprint airborne LiDAR. *Journal of Forest Research*, 10, 135-142.

Takahashi, T., Yamamoto, K., Senda, Y. and Tsuzuku, M., 2005b. Predicting individual stem volumes of sugi (Cryptomeria japonica D. Don) plantations in mountainous areas using small-footprint airborne LiDAR. *Journal of Forest Research*, 10, 305-312.

Takahashi, T., Yamamoto, K. and Senda, Y., 2008a. Comparison of different sampling density data for detecting and measuring individual trees in a mountainous coniferous forest using small-footprint airborne LiDAR. *Journal of Forest Planning*, 13, 249-258.

Takahashi, T., Awaya, Y., Hirata, Y., Furuya, N., Sakai, T. and Sakai, A., 2008b. Effects of flight altitude on LiDAR-derived tree heights in mountainous forests with poor laser penetration rates. *The Photogrammetric Journal of Finland*, 21, 86-96.

Wang, L., Gong, P. and Biging, S., 2004. Individual tree-crown delineation and treetop detection in high-resolution aerial imagery. *Photogrammetric Engineering and Remote Sensing*, 70, 351-357.

Worboys, M. and Duckham, M., 2004. GIS A computing perspective. *CRC PRESS*, Florida, USA, 190-192.

Wulder, M., Niemann, K.O. and Goodenough, D.G., 2000. Local maximum filtering for the extraction of tree locations and basal area from high spatial resolution imagery. *Remote Sensing of Environment*, 73, 103-114.

Yu, X., Hyyppä, J., Hyyppä, H. and Maltamo, M. 2004. Effects of flight altitude on tree height estimation using airborne laser scanning. *International Archives Photogrammetric, Remote Sensing and Spatial Information Science,* 36, part8/w2